Comparison and Reappraisal of Carbon Electrodes for the Voltammetric Detection of Dopamine

ARTICLE *in* ANALYTICAL CHEMISTRY · DECEMBER 2013

Impact Factor: 5.64 · DOI: 10.1021/ac401969q · Source: PubMed

5 AUTHORS, INCLUDING:

Anisha N Patel
Paris Diderot University
13 PUBLICATIONS **259** CITATIONS
SEE PROFILE

Sze-yin Tan
The University of Warwick
5 PUBLICATIONS **44** CITATIONS
SEE PROFILE

Julie V Macpherson
The University of Warwick
175 PUBLICATIONS **5,625** CITATIONS
SEE PROFILE

analytical chemistry

Article

pubs.acs.org/ac

Comparison and Reappraisal of Carbon Electrodes for the Voltammetric Detection of Dopamine

Anisha N. Patel, Sze-yin Tan, Thomas S. Miller, Julie V. Macpherson, and Patrick R. Unwin*

Department of Chemistry, University of Warwick, Coventry CV4 7AL, U.K.

Supporting Information

ABSTRACT: The electro-oxidation of dopamine (DA) is investigated on the unmodified surfaces of five different classes of carbon electrodes: glassy carbon (GC), oxygen-terminated polycrystalline boron-doped diamond (pBDD), edge plane pyrolytic graphite (EPPG), basal plane pyrolytic graphite (BPPG), and the basal surface of highly oriented pyrolytic graphite (HOPG), encompassing five distinct grades with step edge density and coverage varying by more than 2 orders of magnitude. Surfaces were prepared carefully and characterized by a range of techniques, including atomic force microscopy (AFM), field emission scanning electron microscopy (FE-SEM), and Raman spectroscopy. Although pBDD was found to be the least susceptible to surface fouling (even at relatively high DA concentrations), the reaction showed sluggish kinetics on this electrode. In contrast, DA electro-oxidation at pristine basal plane HOPG at concentrations ≤100 μM in 0.15 M PBS, pH 7.2, showed fast kinetics and only minor susceptibility toward surface fouling from DA byproducts, although the extent of HOPG surface contamination by oxidation products increased substantially at higher concentrations (with the response similar on all grades, irrespective of step edge coverage). EPPG also showed a fast response, with little indication of passivation with repeated voltammetric cycling but a relatively high background signal due to the high capacitance of this graphite surface termination. Of all five carbon electrode types, freshly cleaved basal plane HOPG showed the clearest signal (distinct from the background) at low concentrations of DA (<10 μM) as a consequence of the low capacitance. Studies of the electrochemical oxidation of DA in the presence of the common interferents ascorbic acid (AA) and serotonin (5-HT), of relevance to neurochemical analysis, showed that the signals for DA were still clearly and easily resolved at basal plane HOPG surfaces. In the presence of AA, repetitive voltammetry caused products of AA electro-oxidation to adsorb onto the HOPG surface, forming a permselective film that allowed the electrochemical oxidation of DA to proceed unimpeded, while greatly inhibiting the electrochemical response of AA itself. The studies presented provide conclusive evidence that the pristine surface of basal plane HOPG is highly active for the detection of DA, irrespective of the step edge density and method of cleavage, and adds to a growing body of evidence that the basal plane of HOPG is a much more active electrode for many classes of electrode reactions than previously believed.

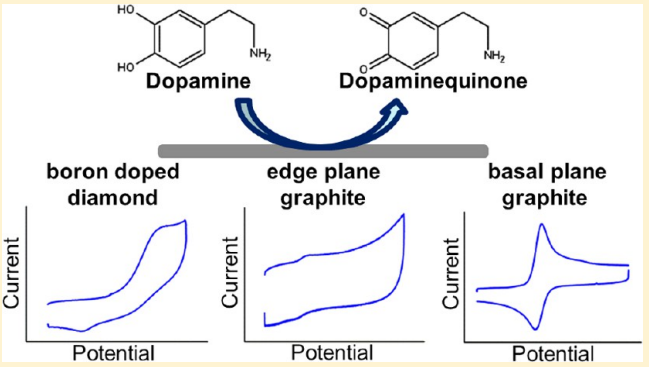

The detection of dopamine (DA) is currently a subject of significant interest. DA is a neurotransmitter that plays an essential role in the function of the central nervous, renal, hormonal, and cardiovascular systems,[1−3] and deficiencies or excesses of DA have been linked to neurological diseases such as Parkinson's disease, schizophrenia, autism, and attention deficit hyperactivity disorder (ADHD).[3−6] The ability to monitor DA levels in vitro and in vivo is highly desirable, from the perspective of gaining a greater understanding of neuronal function[7,8] to developing diagnostic tools.

As neurotransmitters are relatively easily oxidized, electrochemical techniques have been investigated extensively as a means of detection and have been shown to provide both qualitative and quantitative information on DA levels.[9−13] However, major issues in the use of voltammetry and amperometry for DA detection are the stability and sensitivity of the electrode response, especially as adsorbed oxidized products can block electrode surfaces, leading to the deterioration of the signal over time.[14,15] Furthermore, in many practical situations, the in vivo detection of DA can be compromised by competing processes, such as the oxidation of ascorbic acid (AA), uric acid, and serotonin (5-HT), which have similar oxidation potentials and, for some, may be present at much higher concentrations.[16−18] In contrast, DA is present in neural extracellular fluid at relatively low levels.[19−21]

The oxidation of DA occurs via a complex two-electron two-proton transfer process (Figure 1),[5,22,23] which can be represented by a scheme of squares, in which the pathway followed is sensitive to pH.[24,25] At physiological pH, the main electrode product is dopaminequinone, but side reactions lead to the formation of leucodopaminechrome,[26−30] and ultimately,

Received: July 1, 2013
Accepted: November 15, 2013
Published: November 15, 2013

melanin-like compounds are formed, which may inhibit electron transfer (ET) and suppress the sensitivity of the electrode response.[27,28,31] On the other hand, melanin has been shown to form a permselective film on some carbon electrodes, which excludes negatively charged species, such as AA, and in some cases has been shown to enhance the electrochemical response for positively charged molecules, for example DA and 5-HT at physiological pH.[32−34]

Most research into the voltammetric detection of DA has focused on the use of carbon-based electrode materials because of a desirable range of properties, including biocompatibility, chemical inertness, and (in some cases) low background currents, which provide better detection limits.[35−39] However, most carbon electrodes are highly susceptible to fouling (as alluded to above).[7,40,41] The extent and rate of electrode fouling are dependent on the material: glassy carbon (GC) has been shown to foul relatively quickly, while polycrystalline boron doped diamond (pBDD) and edge plane pyrolytic graphite (EPPG) have been reported as being relatively resistant to fouling.[36,42−46]

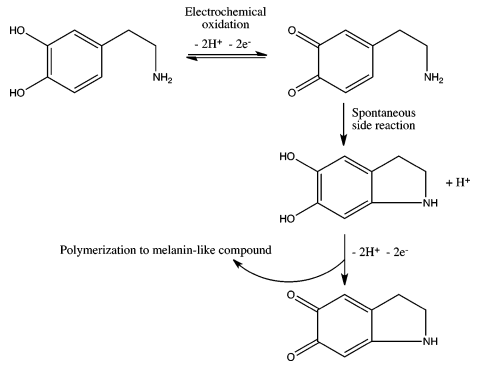

Figure 1. Oxidation scheme for DA at neutral pH (adapted from ref 29).

The goal of this paper is to re-examine and compare the intrinsic activity of various carbon electrodes toward the electrochemical oxidation of DA, not least because of considerable recent insights on the electrochemical behavior of carbon materials revealed by high-resolution electrochemical imaging (see below).[47−53] We compare the activity of GC, pBDD, the basal plane of highly oriented pyrolytic graphite (HOPG), and two orientations of pyrolytic graphite (basal and edge), as the major carbon materials used for electrochemistry. Comparison of graphite and highly doped pBDD is interesting, as these materials differ in carbon structure (sp^2 vs sp^3) but are both semimetallic and possess comparable densities of electronic states (DOS) at the Fermi level, ca. $(2–6) \times 10^{20}$ cm^{-3} eV^{-1}, for potentials and conditions relevant to aqueous electrochemistry.[54,55] GC comprises highly disordered and randomly intertwined

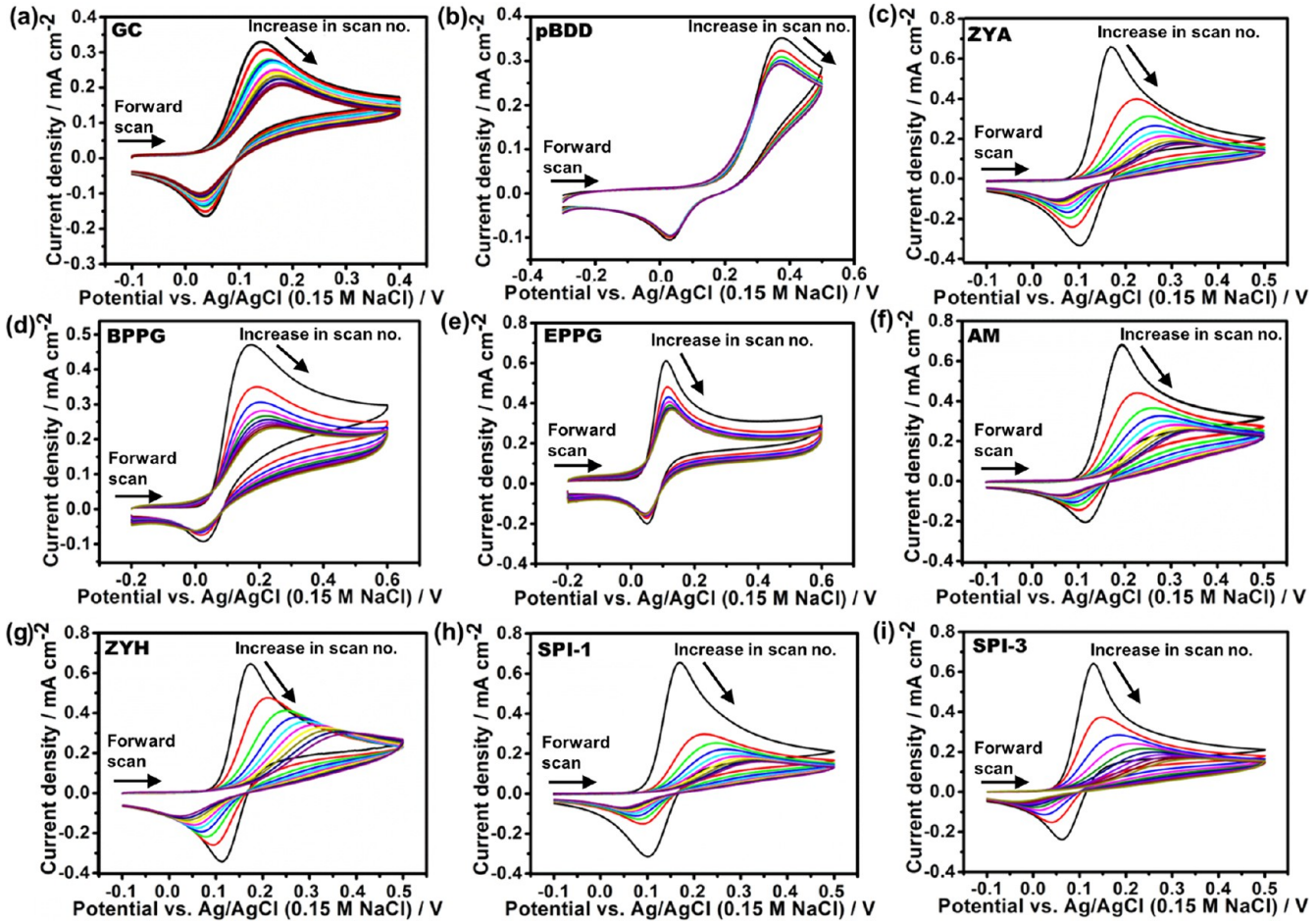

Figure 2. Repetitive cycling for the oxidation of 1 mM DA in 0.15 M PBS, pH 7.2, at 0.1 V s^{-1} with (a) GC, (b) pBDD, (c) ZYA HOPG, (d) BPPG, (e) EPPG, (f) mechanically cleaved AM HOPG (data replotted from ref 53), (g) ZYH HOPG, (h) SPI-1 HOPG, and (i) SPI-3 HOPG. In each case, 10 consecutive scans were run with 5 s intervals between the end of one and the start of the next.

dx.doi.org/10.1021/ac401969q | Anal. Chem. 2013, 85, 11755−11764

ribbons of graphitic planes creating a tight mixture of sp^2 and sp^3 carbon domains;[56] the material is widely considered to possess a DOS comparable to that of metal electrodes, such as gold.[57]

Until recently,[51−53] the traditional consensus was that the basal plane of HOPG either was electrochemically inert[58,59] or was characterized by extremely slow ET kinetics,[60,61] even for simple outer-sphere redox processes. In contrast, step edge sites on the basal surface have been widely considered to promote fast ET kinetics by increasing the standard rate constant in comparison to the basal surface by several orders of magnitude up to 10^7-fold.[58] Electron transfer at step edges is thus considered to be the microscopic process dominating macroscopic voltammetry at basal plane HOPG. However, scanning tunneling spectroscopy studies indicate that the DOS across HOPG is relatively uniform, with an enhancement of the local DOS only at zigzag steps,[62−64] which are the minority step sites in comparison to armchair-terminated steps, where there is no DOS enhancement.[62,63] Moreover, zigzag steps only affect the overall DOS of a graphite surface when the step coverage is very high: i.e., for step spacing <10 nm.[64,65] Step edges have also been reported to promote adsorption and provide fast ET for DA oxidation, while the basal plane is supposedly inert toward adsorption, leading to extremely slow DA oxidation at HOPG, where the step density is low.[7,66,67] Voltammetric analysis of DA on cleaved HOPG has indicated that very high overpotentials are needed, with the forward to reverse peak-to-peak separation (ΔE_p) in cyclic voltammetry (CV) as high as 1.2 V (scan speed 0.2 V s^{-1}).[67] This has been a generally established view that extends to other multistep electrochemical processes of similar classes of molecules.[68] As a consequence, it has generally been recommended to design graphite and carbon fiber electrode surfaces to optimize the step edge density[7,69−73] and to avoid basal plane orientations.

In contrast, recent nanoscale imaging and reactive patterning on HOPG using scanning electrochemical cell microscopy (SECCM) has revealed that both the basal and edge plane sites of HOPG are highly electrochemically active for the oxidation of DA[53] and related compounds,[74] a view that is also supported by recent scanning electrochemical microscopy (SECM) studies, which found DA oxidation to occur readily at the basal plane of HOPG.[50] A key attribute of SECCM is that one can make tens of thousands of measurements in known locations across a surface and correlate the activity with electrode structure at the nanoscale.[75] Our studies showed that the basal surface of high-quality mechanically cleaved HOPG was highly electrochemically active toward DA oxidation.[53] Furthermore, our recent investigations of epinephrine (EP) electro-oxidation on the same high-quality HOPG reached the same conclusion on the intrinsic electroactivity of the graphite basal surface. Importantly, we also showed that step edge density (by comparing the highest quality HOPG with one having a step edge site coverage about 2 orders of magnitude higher) had no noticeable impact on the voltammetry for EP electro-oxidation.[74] In light of these new findings, it is timely to re-examine the electrochemistry of DA on a variety of carbon electrodes, including different grades of HOPG with a wide range of step edge coverage (for comparison with our recent study of mechanically cleaved HOPG of the highest quality[53]), with the aim of understanding structural controls on DA electro-oxidation. This approach identifies the optimal electrode material for voltammetric analysis and leads to new design criteria for carbon electrodes employed for DA (and, more generally, catechol) detection.

EXPERIMENTAL SECTION

Materials and Reagents. All chemicals were used as received, and all solutions were prepared with high-purity Milli-Q reagent water (Millipore Corp.) with resistivity 18.2 MΩ cm at 25 °C. Dopamine hydrochloride, L-(+)-ascorbic acid sodium salt, and phosphate-buffered saline (PBS) solution (pH 7.2) were purchased from Sigma-Aldrich. All solutions were prepared fresh on the day of the experiments and kept in the dark at all times when not in use. The working electrodes employed were as follows: a GC electrode (3 mm diameter) sheathed in PTFE (CH Instruments, Austin, TX), a polycrystalline boron doped diamond (pBDD) electrode (1 mm in diameter and ca. 500 μm thick, sheathed in glass), prepared in house from DIAFILM EA grade material (Element Six Ltd.),[76,77] basal plane HOPG (grades ZYA, ZYH, SPI-1, and SPI-3, from SPI Supplies, West Chester, PA, and an unclassified grade of the highest quality[52] originating from Dr. Arthur Moore at Union Carbide and kindly provided by Prof. R. L. McCreery of the University of Alberta, Canada, hereafter referred to as "AM grade"), and basal plane and edge plane pyrolytic graphite (BPPG and EPPG) (Mersen UK, Teesside). Note that BPPG has the basal graphite plane exposed, but the material has a much smaller crystallite size than HOPG, so that while having basal plane character, the BPPG surface has substantial edge plane character, as we show herein. The average boron doping level of the pBDD material was ca. 5×10^{20} atoms cm^{-3}, above the metallic threshold, and the variation in dopant density between different grains in this material has been reported in recent papers from our group.[55,78]

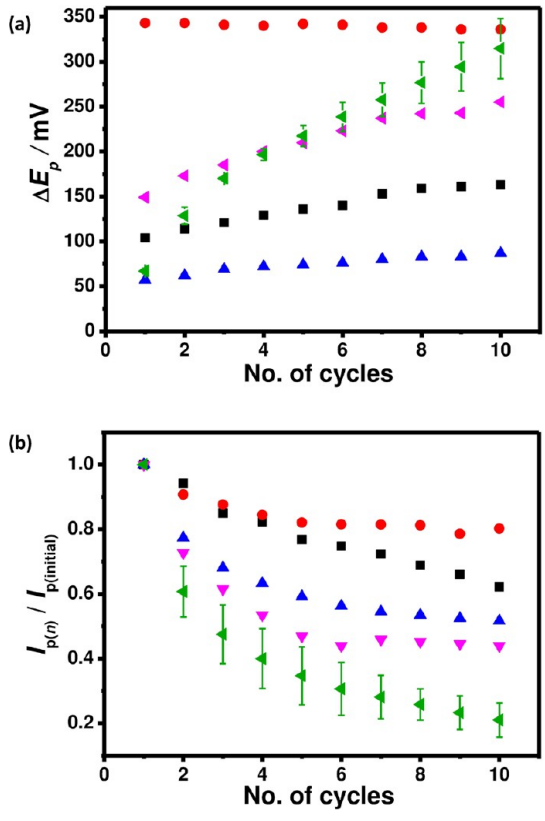

Figure 3. (a) Plot of ΔE_p vs number of cycles and (b) $I_{p(n)}/I_{p(initial)}$ vs number of cycles, *n*, for the electro-oxidation of DA (data in Figure 2): pBDD (red); GC (black); EPPG (blue); BPPG (pink); basal plane HOPG (green). The latter plots show the mean and standard deviation of data for the five grades of HOPG shown in Figure 2.

dx.doi.org/10.1021/ac401969q | Anal. Chem. 2013, 85, 11755−11764

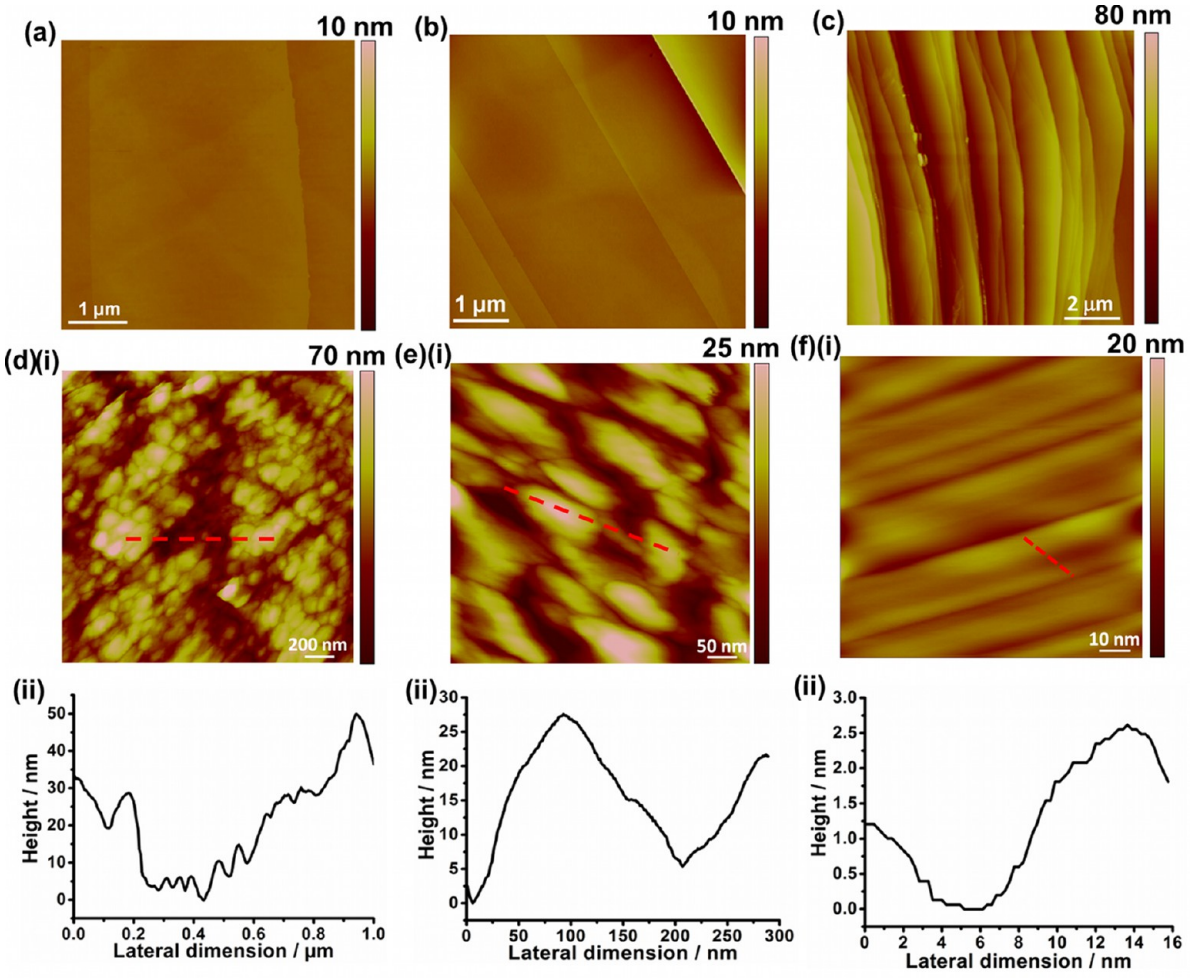

Figure 4. TM-AFM topography images of freshly cleaved HOPG with the following grades: (a) mechanically cleaved AM; (b) ZYA; (c) SPI-3; (d–f) BPPG at different magnifications as (i) topography maps and (ii) cross sections.

Table 1. Step Edge Coverage of HOPG (Five Different Grades) and BPPG

	AM[a] (N = 20)	ZYA[a] (N = 15)	ZYH[a] (N = 10)	SPI-1[a] (N = 14)	SPI-3[b] (N = 10)	BPPG[c] (N = 3)
step density range (μm μm^{-2}) from AFM	0.003–0.12	0.1–0.7	0.5–2.3	0.3–3.6	2.5–21.9	
mean step density (μm μm^{-2})	0.02 ± 0.02	0.5 ± 0.1	1.2 ± 0.6	1.5 ± 0.2	8.0 ± 5.8	
av step-edge coverage (%)	0.09 ± 0.09	0.3 ± 0.25	0.8 ± 0.4	1.7 ± 1.6	30 ± 24	110 ± 5
step-edge coverage range (%)	0.006–0.48	0.03–1	0.2–2.1	0.5–3.4	10.1–78.0	105–120

[a]Data from ref 52. [b]Data from ref 74. [c]Data from this study. HOPG prepared by Scotch tape cleavage except for AM grade, which was mechanically cleaved.

The material was lapped (~nm surface roughness) and subject to a stringent acid clean before encapsulation in glass.

Electrode Fabrication and Preparation. The pBDD-disk electrodes with ohmic back contacts were connected by sealing a disk inside a pulled glass capillary, as described elsewhere.[77] Prior to the electrochemical measurements, GC and pBDD electrodes were polished with alumina slurries (0.05 μm) on soft microfiber polishing pads (MicroCloth, Buehler Ltd.) and then again on clean wet microfiber pads, a recently established optimal method for pBDD surface preparation.[76] For GC we also carried out sonication, followed by soaking in isopropyl alcohol, but saw no difference in the voltammetric response for DA in comparison to polishing on alumina and then on clean wet microfiber pads. HOPG, EPPG, and BPPG were contacted to a silicon wafer, coated with chromium (2 nm) and gold (60 nm), using Acheson Electrodag (Agar Scientific, 1415M). An external electrical contact was created by lowering a metal pin onto the gold surface using a micropositioner; this method also enabled the samples to be secured for ex situ and in situ atomic force microscopy (AFM). The basal plane HOPG surfaces were freshly prepared by gently pressing down single-sided Scotch tape and gently pulling off the top layers, as described elsewhere[51] and as used extensively in the literature.[60,61,66,67,79,80] We compare data obtained on different grades of HOPG using this approach with the characteristics on the highest quality HOPG (AM grade) prepared by mechanical cleavage. EPPG and BPPG surfaces were prepared by polishing with alumina slurries on soft microfiber polishing pads followed by ultrasonication for 10 min and soaking in isopropyl alcohol.

Electrochemistry. Cyclic voltammetry (CV) was carried out in a three-electrode configuration using a potentiostat (CH Instruments Model 750A, Austin, TX). A silver/silver chloride

dx.doi.org/10.1021/ac401969q | Anal. Chem. 2013, 85, 11755–11764

electrode (Ag/AgCl in 0.15 M NaCl) served as the reference, with a Pt counter electrode. The working electrodes were as described above. On freshly cleaved HOPG, unless stated otherwise, a Teflon cell designed in house was used to provide a well-defined 3 mm working area; this is described in detail elsewhere.[52]

Micro-Raman Microscopy. Micro-Raman spectra were collected using a RenishawinVia Raman microscope fitted with a CCD detector and a 633 nm HeNe laser, with a spot size of 3 μm and 5% attenuation.

Field Emission Scanning Electron Microscopy. A Zeiss SUPRA 55 VP FE-SEM instrument with an in-lens detector and a secondary electron emission detector was used to obtain images of EPPG and BPPG.

In Situ Electrochemical AFM. In situ AFM experiments were carried out using a Veeco Bioscope Catalyst AFM, operated in Tapping Mode, using standard silicon nitride tips (NP-type). Electrochemical control of the working electrode was as above, utilizing a CH Instruments potentiostat (Model 800B, Austin, Texas).

RESULTS AND DISCUSSION

Influence of Repetitive Voltammetric Cycling. It is widely appreciated that DA electro-oxidation can lead to rapid fouling and contamination of working electrode surfaces, as highlighted above. Thus, the extent to which the responses of the different carbon electrodes changed during DA electro-oxidation was studied by recording consecutive CVs (typically 10 at 0.1 V s^{-1}), with 5 s intervals between each CV for each electrode. Figure 2 shows typical CVs for repetitive cycling in 1 mM DA (0.15 M PBS, pH 7.2), using the carbon electrodes (a) GC, (b) pBDD, (c) ZYA grade HOPG, (d) BPPG, and (e) EPPG and for comparison (f) mechanically cleaved AM (data from ref 53), (g) ZYH, (h) SPI-1, and (i) SPI-3. Summary data comparing the change in ΔE_p and peak current for the forward scan with voltammetric cycling can be found in Figure 3. The peak current data are presented as $I_{p(n)}/I_{p(initial)}$, where n is the number of cycles and "initial" indicates the first cycle. As the responses for the different grades and preparations of HOPG are rather similar (vide infra), the data for HOPG are the mean and standard deviation of the entire data set for the five different types of HOPG.

It can be seen that the initial CV for each carbon electrode shows the most reversible response, although the extent of reversibility depends on the particular carbon material. On subsequent cycles the response deteriorates on each electrode, but the extent to which this occurs also depends on the electrode.

A few particularly interesting observations can be made from the CVs for these different electrodes. It is noticeable that the responses of the five different grades of basal plane HOPG are closely similar, even though the step edge densities vary by more than 2 orders of magnitude (see Figure 4a–c and Table 1). The initial CV on basal plane HOPG is quite reversible, but the response falls off rapidly with increasing n, with the pattern of blocking fairly insensitive to the step edge density over the wide range considered. The observations are consistent with our recent SECCM study,[53] which showed clearly that DA oxidation occurred rapidly at the basal graphite surface but that the surface was rapidly contaminated by reaction products, in line with the scheme in Figure 1.

Step edge coverage analysis carried out in recent studies[52,74] on different HOPG grades, namely AM (mechanically cleaved),

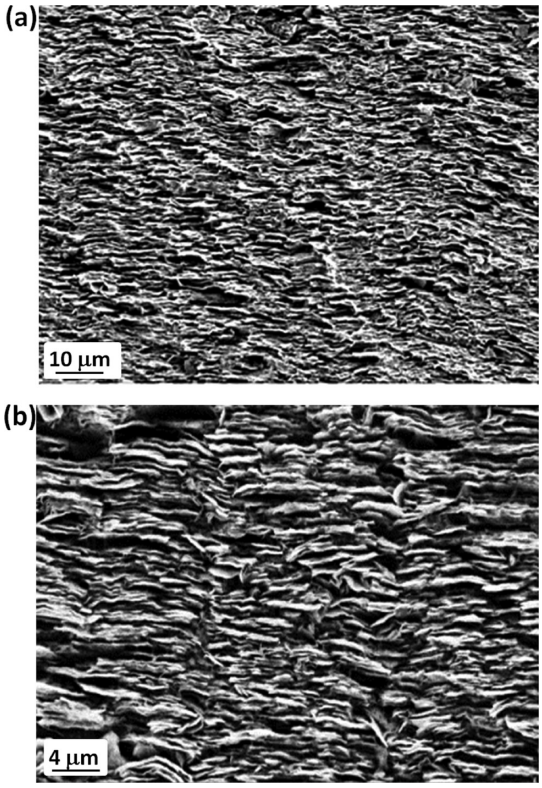

Figure 5. FE-SEM images of freshly prepared EPPG.

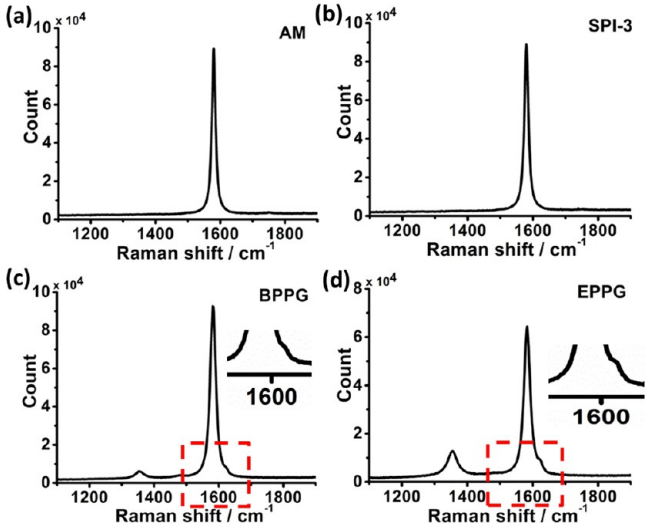

Figure 6. Raman spectra run on freshly prepared (a) mechanically cleaved AM grade HOPG, (b) Scotch tape cleaved SPI-3 grade HOPG, (c) BPPG, and (d) EPPG.

ZYA, ZYH, SPI-1, and SPI-3, are summarized in Table 1. Step edge character is defined in two ways: (i) as the step edge length (μm) in unit area of the surface (μm^2), not taking account of the step height (monolayer, bilayer, etc.) and (ii) as the total step edge area per unit geometric area of the surface, which takes account of different step edge heights.[52] By both measures these data highlight that the different HOPG grades vary in step edge coverage by more than 2 orders of magnitude. Step height histograms for the five HOPG grades show that all surfaces except SPI-3 exhibit mainly monolayer (and bilayer) steps, with SPI-3 revealing predominantly multiplayer steps

dx.doi.org/10.1021/ac401969q | Anal. Chem. 2013, 85, 11755–11764

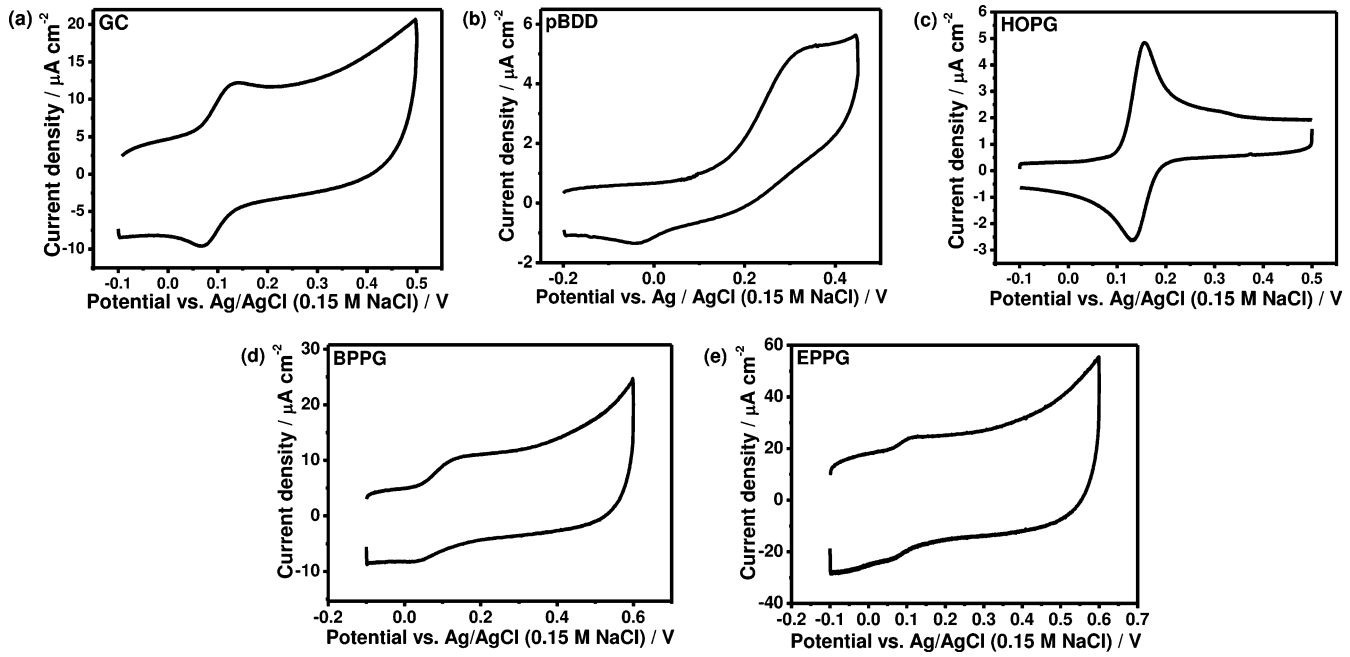

Figure 7. CVs for the oxidation of 10 μM DA in 0.15 M PBS, pH 7.2, at 0.1 V s^{-1} on (a) GC, (b) pBDD, (c) basal plane HOPG (ZYA grade), (d) BPPG, and (e) EPPG.

(see the Supporting Information, section S1). New analysis from this study on freshly prepared BPPG shows the projected surface actually has more edge plane than basal plane character. This quantitative analysis is apparent visually in Figure 4, which shows typical TM-AFM topography images of mechanically cleaved AM (a) and Scotch tape cleaved ZYA (b) and SPI-3 (c) HOPG, together with views and cross sections of BPPG at different magnifications (d, e). For BPPG, the cross sections taken from the AFM images show large oval domains on the basal surface (d(ii)) up to 30 nm in height (e(ii)), with the sides of these features consisting of an abundance of step edges (f(ii)).

In light of the structural details presented above, it is interesting to compare the responses for HOPG with those of BPPG. Apart from the initial cycle, where the voltammetric response for BPPG seems slightly more sluggish than for HOPG, the subsequent responses are broadly similar, but the deterioration of the response for HOPG is slightly more severe than for BPPG. As we have shown elsewhere,[53] and as we illustrate further herein, the deterioration in the CV response with cycling is due to the accumulation of side products (Figure 1) on the surface. Evidently, surface structure plays a role, with HOPG (characterized by extensive basal terraces) showing more extensive deterioration of the voltammetric response than BPPG (with shorter terraces).

Interestingly, EPPG electrodes appear much less susceptible to blocking than the basal surfaces, as evidenced by the data for the EPPG electrode (Figures 2e and 3). Although the initial scan (with ΔE_p = 57 mV) is as reversible as that on basal plane HOPG, ΔE_p increases by only 30 mV over the course of 10 cycles. Furthermore, although I_p decreases appreciably between the first and second scans, the peak current magnitude then stabilizes. FE-SEM images of EPPG are shown in Figure 5. These show that the surface is terminated by the edges of graphite platelets, such that while there is substantial edge plane character, there is also a considerable amount of basal surface, but the terraces are very short compared to those of BPPG. The shorter terrace length and extensive edge plane

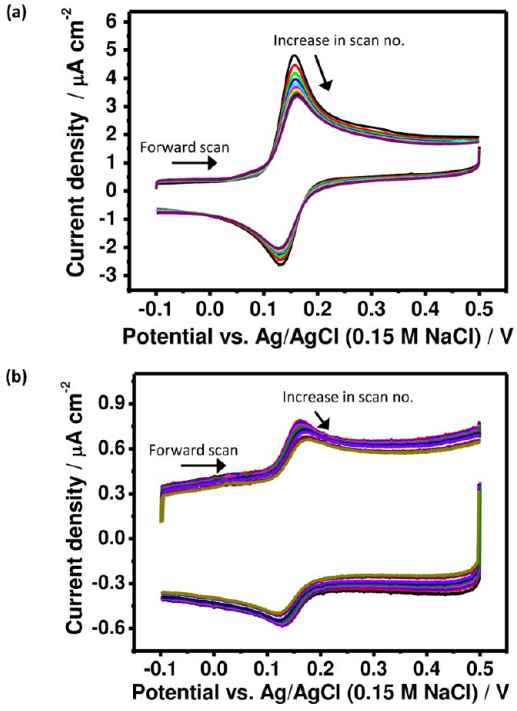

Figure 8. Repetitive CVs for the oxidation of DA at concentrations of (a) 10 μM and (b) 1 μM (0.15 M PBS, pH 7.2, at 0.1 V s^{-1}) on basal plane HOPG (ZYA).

character appear to make this orientation of graphite relatively immune to blocking during DA voltammetry.

The structural features evident in the different graphite materials described above are manifested in the Raman spectra, shown in Figure 6 for (a) mechanically cleaved AM HOPG, (b) Scotch tape cleaved SPI-3 HOPG, (c) BPPG, and (d) EPPG. The spectra for the two HOPG grades, showing a single peak at 1589 cm^{-1}, corresponding to the G band, are indicative of high-quality sp^2 carbon. EPPG and BPPG also show not only a

dx.doi.org/10.1021/ac401969q | Anal. Chem. 2013, 85, 11755−11764

prominent G band but also a D band at 1360 cm^{-1}, which is indicative of sp^3 carbon and can be attributed to the presence of significant defects and step edges.[81] The shoulder on the G bands in the spectra for EPPG and BPPG, shown as the inset zoom to this region in Figure 6, referred to as the D′ or D* band, further highlights the considerable disorder in these graphite materials (EPPG and BPPG), due to intercalation or delamination of graphite planes and a significant exposure of step edges.[66,82] Evidently, in agreement with the microscopy analysis, the DA voltammetric response during cycling deteriorates least when the amount of disorder in graphite is greater (as measured by the G/D ratio): the response (at 1 mM DA) deteriorates quickly on HOPG, followed by BPPG and finally EPPG.

The GC electrode, which is rich in oxygen-containing moieties[57] and disordered graphite, also shows some resistance toward surface deactivation but not to the same extent as EPPG, with the ΔE_p value increasing by ~60 mV over the course of 10 cycles and I_p decreasing monotonically to ~60% of the initial value (Figures 2e and 3). Finally, pBDD shows highly irreversible voltammetry but the most reproducible response with the number of cycles (Figures 2b and 3). After 10 cycles, ΔE_p increases by only ~5 mV and although I_p decreases by 20% in the first four cycles, the I_p value is then stable (Figure 3). A comparison of the data for pBDD and basal plane HOPG is further illuminating because, as highlighted at the beginning of this paper, these electrode materials have broadly similar DOS, yet the carbon structures are very different. Evidently, it would appear that the basal sp^2 surface promotes strong coupling of DA to the electrode, leading not only to fast ET but also to blocking of the electrode by products of the reaction. In contrast, the adsorption of DA, and products of the oxidation reaction, at pBDD appears to be much less extensive, which ties in with the electrochemical kinetics being slower and the pBDD remaining relatively immune to passivation.

Low-Concentration Detection of DA. Although many voltammetric studies of DA electro-oxidation tend to focus on millimolar levels,[31,67,83,84] lower level detection is much more relevant to practical applications, and so we next consider CVs for DA oxidation at a concentration of 10 μM on freshly prepared surfaces of the five different classes of carbon electrode materials. Some of the data are summarized in Figure 7, which shows that although all electrodes were able to detect DA at 10 μM, the precision of the measurement varies substantially with the electrode material. At this concentration level, the background response of the electrode material becomes particularly important in determining the sensitivity of detection. Thus, although the response is close to reversible on GC (Figure 7a), the large capacitance current makes the signal more difficult to discern than on HOPG. The response on pBDD (Figure 7b) is again irreversible, but the low intrinsic capacitance of pBDD[55] gives rise to a low background current, so that the signal for DA oxidation is easily seen. A comparison of the three different types of graphite materials (HOPG, BPPG, and EPPG) highlights the superior signal of basal plane HOPG as a consequence of the very low capacitance[52,60,85] in comparison to both BPPG and EPPG. Indeed, at a lower DA concentration of 1 μM, only basal plane HOPG showed a clear voltammetric response at this scan rate (vide infra). All peak current magnitudes are similar at low concentrations (and scale reasonably with concentration to the current magnitudes in the first voltammetric cycle at 1 mM; vide supra), indicating the process is diffusion-controlled, but the extent to which the signal can be observed is dependent on the surface.

It is evident when comparing the initial responses in Figure 2 with those in Figure 7 that DA electro-oxidation appears to be much more reversible at low concentration and is highly reversible on the various graphite electrodes and GC. A primary factor in this different behavior is that the lower flux of DA to the electrode, as a consequence of the lower concentration, leads to much slower formation and accumulation of blocking side products, which influence the voltammetric response even in the first scan at higher concentration.

As HOPG was evidently the optimal material for DA detection at low concentrations (on the basis of a comparison of initial responses of the different electrodes), we were particularly interested in elucidating the time-dependent behavior of this electrode during CV cycling. The extent of surface fouling on the basal plane of HOPG was significantly reduced when the DA concentration was decreased. Ten CVs (0.1 V s^{-1}) recorded at 5 s intervals in 100 μM DA (Supporting Information, S2)

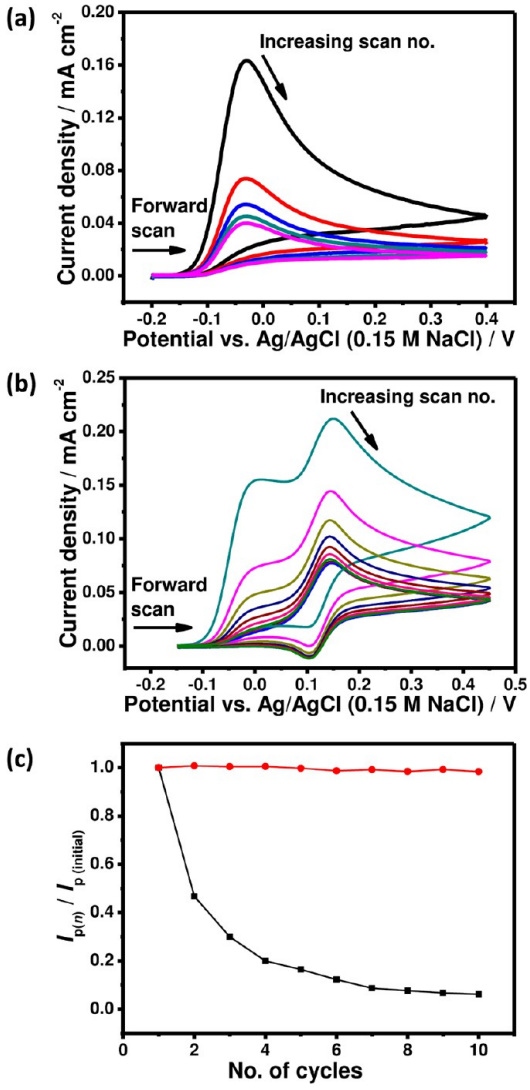

Figure 9. Repetitive CVs for the oxidation of (a) 500 μM AA and (b) 500 μM AA and 100 μM DA, with 0.15 M PBS, pH 7.2, at 0.1 V s^{-1} on basal plane HOPG (ZYA). CVs were run at 5 s intervals. (c) Plot highlighting the change in peak current with successive cycling in (b) for AA (black) and DA (red).

dx.doi.org/10.1021/ac401969q | Anal. Chem. 2013, 85, 11755−11764

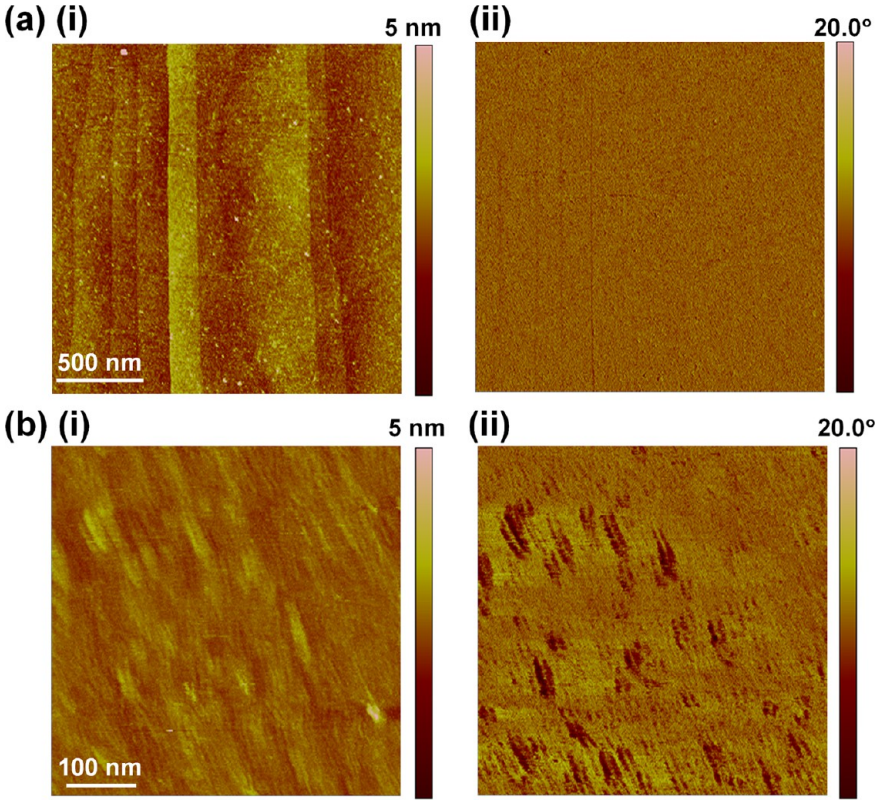

Figure 10. In situ (a) 2 × 2 μm and (b) 500 × 500 nm AFM images of basal plane HOPG after one potential cycle between −0.2 and +0.6 V at 0.1 V s^{-1} in a solution containing 500 μM AA (0.15 M PBS, pH 7.2).

and in 10 μM and 1 μM DA (Figure 8) clearly show that the electrochemical reversibility of DA electro-oxidation is maintained during cycling as the DA concentration is progressively lowered. Analysis of the change in I_p and ΔE_p as a function of cycle number (Supporting Information, Figure S2) illustrates this point. In particular, the change in ΔE_p is much greater at 1 mM DA (~220 mV increase over 10 cycles) in comparsion to 100 μM (~10 mV increase over 10 cycles) and 10 μM DA (a change of ca. 5−8 mV over 10 cycles). It should be noted that at 100 μM DA and lower concentrations, the initial ΔE_p value is ca. 30 mV, which is similar to that found on GC surfaces treated to minimize surface impurities by fracturing or laser activation,[24,86,87] from which it was concluded that defects were needed to promote DA electro-oxidation.[88] The studies herein show that very similar behavior can be observed on pristine HOPG surfaces that contain few step edges.[52] Analysis of the change of I_p with n at different DA levels confirms this behavior. I_p decreases by 75% at 1 mM DA, after 10 cycles, in comparison to 40% at 100 μM DA (10 cycles) and a 25% decrease at 10 μM DA (10 cycles). Significantly, CVs recorded with 1 μM DA on ZYA grade HOPG show a clear response with minimal electrode blocking over time (Figure 8b).

Interference Study. As a major problem encountered when attempting to detect DA in practical situations is the interference from the oxidation of other species present, such as AA, the detection of DA was investigated in the presence of AA. HOPG was selected for these studies, given the attributes identified above, particularly for DA detection at trace levels. First, CVs were run with 500 μM AA (0.15 M PBS, pH 7.2) at 0.1 V s^{-1}, on basal plane HOPG (Figure 9a). The oxidation of AA involves an irreversible two-electron two-proton transfer, and there is no peak when the potential sweep is reversed. As observed with DA electro-oxidation at high concentrations, a large decrease in I_p is observed with successive potential cycling, indicating fouling of the surface by AA oxidation products.

With the addition of 100 μM DA to the solution, on a freshly cleaved HOPG surface, the resulting voltammogram showed two clear peaks (Figure 9b), which can be identified as being due to the oxidation of AA (I) and DA (II). During potential cycling, the AA peak rapidly decreased but, surprisingly, there was no noticeable change in the I_p values (forward and reverse sweeps) and ΔE_p for DA oxidation (Figure 9a). This is shown more clearly in a plot of $I_{p(n)}/I_{p(initial)}$ against number of cycles (Figure 9c). It can be seen that, after 10 consecutive cycles, the AA signal has almost completely disappeared but the DA signal remains relatively constant. Indeed, the voltammetric signature after extensive cycling for DA is even clearer with AA present than without it (cf. Figure 9 and the Supporting Information, Figure S2a).

The data suggest the formation of a film that possesses a negative charge, thereby excluding AA but allowing DA electrochemistry. Film formation was confirmed by in situ AFM on freshly cleaved basal plane HOPG in a 500 μM AA solution (0.15 M PBS, pH 7.2). After performing one potential cycle in the range −0.2 to +0.6 V, at 0.1 V s^{-1}, topographical and phase images (Figure 10a) show strong evidence for adsorbed species across basal terraces and edge plane sites of the HOPG surface. A zoom to a smaller region (Figure 10b) shows this film to be continuous, explaining the strong barrier effect.

A further preliminary study was carried out on DA electro-oxidation on HOPG (ZYA) in the presence of 5-HT, another redox-active neurotransmitter that is also a common interfering agent in the detection of DA.[89−91] The CV provided in Figure S3 in the Supporting Information shows two clear peaks for the two species that are clearly distinguishable.

dx.doi.org/10.1021/ac401969q | *Anal. Chem.* 2013, 85, 11755−11764

CONCLUSIONS

The electrochemical response of DA at prominent carbon electrodes has been re-evaluated and analyzed. Electrode surfaces were carefully prepared and characterized by a range of techniques. The most striking result, in contrast to previous voltammetric studies, is that the freshly prepared and unmodified basal plane of HOPG provides an electrode surface on which DA oxidation occurs readily, supporting evidence from recent microscopic studies.[50,53] Step edges are not required to catalyze the electro-oxidation of DA. A comparison between DA voltammetry on basal plane HOPG in comparison to polished EPPG (over the range of concentrations 1 μM to 1 mM) clearly shows that HOPG provides the clearest analytical signal. Significantly, freshly cleaved HOPG yields fast electrochemistry for the oxidation of DA (at concentrations below 10 μM) and the best voltammetric signal to background current in comparison to the four other types of carbon-based electrodes studied herein. However, at concentrations above 100 μM, the basal plane of HOPG is very susceptible to blocking by dopaminergic products. This could explain, at least in part, the behavior seen in past work, which has seen sluggish kinetics but which has tended to focus on higher DA concentrations.

It is also significant that the voltammetric signal between AA and DA can be easily resolved on HOPG, without any electrode surface modification, and that the electro-oxidation of AA leads to the formation of a thin film that selectively excludes anions, such as AA, but allows DA electro-oxidation to proceed unimpeded.

Of the other electrodes, the response of pBDD is noteworthy. Although the electro-oxidation process is highly irreversible, this electrode shows minimal deterioration of the voltammetric response, even at relatively high DA concentrations. Coupled with the low intrinsic capacitance of pBDD, trace level detection of DA at pBDD is opened up. The very different responses of pBDD and HOPG are further illuminating in terms of fundamental electrochemistry. These materials have broadly similar DOS, yet the electro-oxidation of DA is much faster on basal plane HOPG in comparison with pBDD, and the reaction is blocked by products of the electro-oxidation much more rapidly on HOPG. This suggests the strong adsorption and electronic coupling of DA to the graphitic surfaces, as well as strong adsorption of reaction products, which ultimately block the reaction.

ASSOCIATED CONTENT

Supporting Information

Text and figures giving a summary of step edge analysis on basal plane HOPG by AFM, the effect of DA concentration on voltammetry at HOPG, and the interference effect of 5-HT on DA voltammetry. This material is available free of charge via the Internet at http://pubs.acs.org.

AUTHOR INFORMATION

Corresponding Author

*P.R.U.: e-mail, p.r.unwin@warwick.ac.uk; fax, +442476524112.

Notes

The authors declare no competing financial interest.

ACKNOWLEDGMENTS

We are grateful to the European Research Council (ERC-2009-AdG 247143-QUANTIF) and EPSRC for a studentship to A.N.P. (Analytical Fund EP/F064861/1e). Some equipment used in this research was obtained through Birmingham Science City with support from Advantage West Midlands and the European Regional Development Fund.

REFERENCES

(1) Weng, J.; Xue, J. M.; Wang, J.; Ye, J. S.; Cui, H. F.; Sheu, F. S.; Zhang, Q. Q. *Adv. Funct. Mater.* **2005**, *15* (4), 639−647.
(2) Barras, A.; Lyskawa, J.; Szunerits, S.; Woisel, P.; Boukherroub, R. *Langmuir* **2011**, *27* (20), 12451−12457.
(3) Shepherd, G. M., *Neurobiology*, 2nd ed.; Oxford University Press: Oxford, U.K., 1988.
(4) Venton, B. J.; Wightman, R. M. *Anal. Chem.* **2003**, *75* (19), 414a−421a.
(5) Wu, K.; Fei, J.; Hu, S. *Anal. Biochem.* **2003**, *318* (1), 100−106.
(6) Andersen, S. L.; Teicher, M. H. *Neurosci. Biobehav. Rev.* **2000**, *24* (1), 137−141.
(7) Bath, B. D.; Michael, D. J.; Trafton, B. J.; Joseph, J. D.; Runnels, P. L.; Wightman, R. M. *Anal. Chem.* **2000**, *72* (24), 5994−6002.
(8) Swamy, B. E.; Venton, B. J. *Analyst* **2007**, *132* (9), 876−884.
(9) Colliver, T. L.; Ewing, A. G. Electrochemical detection of Neurotransmitters. *In Encyclopedia of Analytical Chemistry*; Wiley: Chichester, U.K., 2006; Vol. *11*, pp 9958−9983.
(10) Berduque, A.; Zazpe, R.; Arrigan, D. W. *Anal. Chim. Acta* **2008**, *611* (2), 156−162.
(11) Makos, M. A.; Kim, Y. C.; Han, K. A.; Heien, M. L.; Ewing, A. G. *Anal. Chem.* **2009**, *81* (5), 1848−54.
(12) Park, J.; Quaiserova-Mocko, V.; Patel, B. A.; Novotny, M.; Liu, A.; Bian, X.; Galligan, J. J.; Swain, G. M. *Analyst* **2008**, *133* (1), 17−24.
(13) Gerhardt, G.; Adams, R. N. *Anal. Chem.* **1982**, *54* (14), 2618−2620.
(14) Lin, X. Q.; Zhang, L. *Anal. Lett.* **2001**, *34* (10), 1585−1601.
(15) Raj, C. R.; Okajima, T.; Ohsaka, T. *J. Electroanal. Chem.* **2003**, *543* (2), 127−133.
(16) Sun, C. L.; Lee, H. H.; Yang, J. M.; Wu, C. C. *Biosens. Bioelectron.* **2011**, *26* (8), 3450−3455.
(17) Liu, Q.; Zhu, X.; Huo, Z.; He, X.; Liang, Y.; Xu, M. *Talanta* **2012**, *97*, 557−562.
(18) Behpour, M.; Ghoreishi, S. M.; Honarmand, E.; Salavati-Niasari, M. *Analyst* **2011**, *136* (9), 1979−1986.
(19) Zen, J. M.; Chen, I. L. *Electroanalysis* **1997**, *9* (7), 537−540.
(20) Hou, S. F.; Kasner, M. L.; Su, S. J.; Patel, K.; Cuellari, R. *J. Phys. Chem. C* **2010**, *114* (35), 14915−14921.
(21) Popa, E.; Notsu, H.; Miwa, T.; Tryk, D. A.; Fujishima, A. *Electrochem. Solid-State Lett.* **1999**, *2* (1), 49−51.
(22) Zhao, Y.; Gao, Y.; Zhan, D.; Liu, H.; Zhao, Q.; Kou, Y.; Shao, Y.; Li, M.; Zhuang, Q.; Zhu, Z. *Talanta* **2005**, *66* (1), 51−57.
(23) Chen, S.-M.; Peng, K.-T. *J. Electroanal. Chem.* **2003**, *547* (2), 179−189.
(24) Poon, M.; McCreery, R. L. *Anal. Chem.* **1986**, *58* (13), 2745−2750.
(25) Deakin, M. R.; Wightman, R. M. *J. Electroanal. Chem. Interfacial Electrochem.* **1986**, *206* (1−2), 167−177.
(26) Zhao, H.; Zhang, Y. Z.; Yuan, Z. B. *Analyst* **2001**, *126* (3), 358−360.
(27) Hou, S.; Zheng, N.; Feng, H.; Li, X.; Yuan, Z. *Anal. Biochem.* **2008**, *381* (2), 179−184.
(28) Bernsmann, F.; Ball, V.; Addiego, F.; Ponche, A.; Michel, M.; Gracio, J. J.; Toniazzo, V.; Ruch, D. *Langmuir* **2011**, *27* (6), 2819−2825.
(29) Hawley, M. D.; Tatawawadi, S. V.; Piekarski, S.; Adams, R. N. *J. Am. Chem. Soc.* **1967**, *89* (2), 447−450.
(30) Lane, R. F.; Hubbard, A. T. *Anal. Chem.* **1976**, *48* (9), 1287−1293.
(31) Alwarappan, S.; Butcher, K. S. A.; Wong, D. K. Y. *Sens. Actuators B* **2007**, *128* (1), 299−305.
(32) Rubianes, M. D.; Arribas, A. S.; Bermejo, E.; Chicharro, M.; Zapardiel, A.; Rivas, G. *Sens. Actuators B* **2010**, *144* (1), 274−279.

(33) Rubianes, M. D.; Rivas, G. A. *Anal. Chim. Acta* **2001**, *440* (2), 99−108.
(34) Li, Y.; Liu, M.; Xiang, C.; Xie, Q.; Yao, S. *Thin Solid Films* **2006**, *497* (1−2), 270−278.
(35) Wen, X. L.; Jia, Y. H.; Liu, Z. L. *Talanta* **1999**, *50* (5), 1027−1033.
(36) Kachoosangi, R. T.; Compton, R. G. *Anal. Bioanal. Chem.* **2007**, *387* (8), 2793−2800.
(37) McCreery, R. L. *Chem. Rev.* **2008**, *108* (7), 2646−2687.
(38) Jacobs, C. B.; Vickrey, T. L.; Venton, B. J. *Analyst* **2011**, *136* (17), 3557−3565.
(39) Zachek, M. K.; Hermans, A.; Wightman, R. M.; McCarty, G. S. *J. Electroanal. Chem.* **2008**, *614* (1−2), 113−120.
(40) Bath, B. D.; Martin, H. B.; Wightman, R. M.; Anderson, M. R. *Langmuir* **2001**, *17* (22), 7032−7039.
(41) Harreither, W.; Trouillon, R.; Poulin, P.; Neri, W.; Ewing, A. G.; Safina, G. *Anal. Chem.* **2013**, *85* (15), 7447−53.
(42) Swain, G. M.; Hupert, M.; Muck, A.; Wang, R.; Stotter, J.; Cvackova, Z.; Haymond, S.; Show, Y. *Diamond Relat. Mater.* **2003**, *12* (10−11), 1940−1949.
(43) Fujishima, A.; Shin, D.; Tryk, D. A.; Merkoci, A.; Wang, J. *Electroanalysis* **2005**, *17* (4), 305−311.
(44) Rao, T. N.; Fujishima, A. *Diamond Relat. Mater.* **2000**, *9* (3−6), 384−389.
(45) Banks, C. E.; Compton, R. G. *Analyst* **2005**, *130* (9), 1232−1239.
(46) Trouillon, R.; O'Hare, D. *Electrochim. Acta* **2010**, *55* (22), 6586−6595.
(47) Anne, A.; Cambril, E.; Chovin, A.; Demaille, C.; Goyer, C. *ACS Nano* **2009**, *3* (10), 2927−2940.
(48) Williams, C. G.; Edwards, M. A.; Colley, A. L.; Macpherson, J. V.; Unwin, P. R. *Anal. Chem.* **2009**, *81* (7), 2486−2495.
(49) Frederix, P. L.; Bosshart, P. D.; Akiyama, T.; Chami, M.; Gullo, M. R.; Blackstock, J. J.; Dooleweerdt, K.; de Rooij, N. F.; Staufer, U.; Engel, A. *Nanotechnology* **2008**, *19* (38), 384004.
(50) Lhenry, S.; Leroux, Y. R.; Hapiot, P. *Anal. Chem.* **2012**, *84* (17), 7518−7524.
(51) Lai, S. C. S.; Patel, A. N.; McKelvey, K.; Unwin, P. R. *Angew. Chem., Int. Ed.* **2012**, *51* (22), 5405−5408.
(52) Patel, A. N.; Collignon, M. G.; O'Connell, M. A.; Hung, W. O.; McKelvey, K.; Macpherson, J. V.; Unwin, P. R. *J. Am. Chem. Soc.* **2012**, *134* (49), 20117−20130.
(53) Patel, A. N.; McKelvey, K.; Unwin, P. R. *J. Am. Chem. Soc.* **2012**, *134* (50), 20246−20249.
(54) Gerischer, H.; Mcintyre, R.; Scherson, D.; Storck, W. *J. Phys. Chem.* **1987**, *91* (7), 1930−1935.
(55) Patten, H. V.; Meadows, K. E.; Hutton, L. A.; Iacobini, J. G.; Battistel, D.; McKelvey, K.; Colburn, A. W.; Newton, M. E.; Macpherson, J. V.; Unwin, P. R. *Angew. Chem., Int. Ed. Engl.* **2012**, *51* (28), 7002−7006.
(56) Salimi, A.; Banks, C. E.; Compton, R. G. *Analyst* **2004**, *129* (3), 225−228.
(57) McCreery, R. L. *Chem. Rev.* **2008**, *108* (7), 2646−2687.
(58) Davies, T. J.; Hyde, M. E.; Compton, R. G. *Angew. Chem.* **2005**, *117* (32), 5251−5256.
(59) Davies, T. J.; Moore, R. R.; Banks, C. E.; Compton, R. G. *J. Electroanal. Chem.* **2004**, *574* (1), 123−152.
(60) McDermott, M. T.; Kneten, K.; McCreery, R. L. *J. Phys. Chem.* **1992**, *96* (7), 3124−3130.
(61) Cline, K. K.; Mcdermott, M. T.; McCreery, R. L. *J. Phys. Chem.* **1994**, *98* (20), 5314−5319.
(62) Kobayashi, Y.; Fukui, K.; Enoki, T.; Kusakabe, K. *Phys. Rev. B* **2006**, *73*, 12.
(63) Kobayashi, Y.; Kusakabe, K.; Fukui, K.; Enoki, T. *Phys. E* **2006**, *34* (1−2), 678−681.
(64) Niimi, Y.; Matsui, T.; Kambara, H.; Tagami, K.; Tsukada, M.; Fukuyama, H. *Phys. Rev. B* **2006**, *73*, 8.
(65) Nakada, K.; Fujita, M.; Dresselhaus, G.; Dresselhaus, M. S. *Phys. Rev. B* **1996**, *54* (24), 17954−17961.
(66) Bowling, R. J.; Packard, R. T.; McCreery, R. L. *J. Am. Chem. Soc.* **1989**, *111* (4), 1217−1223.
(67) Kneten, K. R.; McCreery, R. L. *Anal. Chem.* **1992**, *64* (21), 2518−2524.
(68) McDermott, M. T.; McCreery, R. L. *Langmuir* **1994**, *10* (11), 4307−4314.
(69) Banks, C. E.; Compton, R. G. *Analyst* **2006**, *131* (1), 15−.
(70) Heien, M. L.; Phillips, P. E.; Stuber, G. D.; Seipel, A. T.; Wightman, R. M. *Analyst* **2003**, *128* (12), 1413−1419.
(71) Brajter-Toth, A.; el-Nour, K. A.; Cavalheiro, E. T.; Bravo, R. *Anal. Chem.* **2000**, *72* (7), 1576−84.
(72) Strand, A. M.; Venton, B. J. *Anal. Chem.* **2008**, *80* (10), 3708−3715.
(73) Takmakov, P.; Zachek, M. K.; Keithley, R. B.; Walsh, P. L.; Donley, C.; McCarty, G. S.; Wightman, R. M. *Anal. Chem.* **2010**, *82* (5), 2020−2028.
(74) Patel, A. N.; Tan, S. Y.; Unwin, P. R. *Chem. Commun.* **2013**, *49*, 8776−8778.
(75) Snowden, M. E.; Güell, A. G.; Lai, S. C. S.; McKelvey, K.; Ebejer, N.; O'Connell, M. A.; Colburn, A. W.; Unwin, P. R. *Anal. Chem.* **2012**, *84* (5), 2483−2491.
(76) Hutton, L. A.; Iacobini, J. G.; Bitziou, E.; Channon, R. B.; Newton, M. E.; Macpherson, J. V. *Anal. Chem.* **2013**, *85* (15), 7230−7240.
(77) Hutton, L.; Newton, M. E.; Unwin, P. R.; Macpherson, J. V. *Anal. Chem.* **2009**, *81* (3), 1023−1032.
(78) Patten, H. V.; Lai, S. C.; Macpherson, J. V.; Unwin, P. R. *Anal. Chem.* **2012**, *84* (12), 5427−5432.
(79) Liu, H.; Favier, F.; Ng, K.; Zach, M. P.; Penner, R. M. *Electrochim. Acta* **2001**, *47* (5), 671−677.
(80) Ji, X.; Banks, C. E.; Crossley, A.; Compton, R. G. *ChemPhysChem* **2006**, *7* (6), 1337−1344.
(81) Wang, Y.; Alsmeyer, D. C.; McCreery, R. L. *Chem. Mater.* **1990**, *2* (5), 557−563.
(82) Pimenta, M. A.; Dresselhaus, G.; Dresselhaus, M. S.; Cancado, L. G.; Jorio, A.; Saito, R. *Phys. Chem. Chem. Phys.* **2007**, *9* (11), 1276−1291.
(83) Wang, J. X.; Li, M. X.; Shi, Z. J.; Li, N. Q.; Gu, Z. N. *Electroanalysis* **2002**, *14* (3), 225−230.
(84) Roy, P. R.; Okajima, T.; Ohsaka, T. *Bioelectrochemistry* **2003**, *59* (1−2), 11−19.
(85) Rice, R. J.; McCreery, R. L. *Anal. Chem.* **1989**, *61* (15), 1637−1641.
(86) Allred, C. D.; McCreery, R. L. *Anal. Chem.* **1992**, *64* (4), 444−448.
(87) DuVall, S. H.; McCreery, R. L. *Anal. Chem.* **1999**, *71* (20), 4594−4602.
(88) DuVall, S. H.; McCreery, R. L. *J. Am. Chem. Soc.* **2000**, *122* (28), 6759−6764.
(89) Jackson, B. P.; Dietz, S. M.; Wightman, R. M. *Anal. Chem.* **1995**, *67* (6), 1115−1120.
(90) Wang, Z. H.; Liang, Q. L.; Wang, Y. M.; Luo, G. A. *J. Electroanal. Chem.* **2003**, *540*, 129−134.
(91) Li, Y. X.; Huang, X.; Chen, Y. L.; Wang, L.; Lin, X. Q. *Microchim. Acta* **2009**, *164* (1−2), 107−112.